X-band Radar based SLAM in Singapore's Off-shore Environment

John Mullane, Samuel Keller[†], Akshay Rao, Martin Adams, Anthony Yeo[§],
Franz S. Hover[‡] and Nicholas M. Patrikalakis[‡]

School of Electrical & Electronic Engineering, Nanyang Technological University, Singapore
[†]*Swiss Federal Institute of Technology, Switzerland*
[§]*SMART Centre, National University of Singapore, Singapore*
[‡]*Massachusetts Institute of Technology, USA*
{*jsmullane,aksh0010,eadams*}*@ntu.edu.sg*
[†]*kellers@ethz.ch*, [§]*anthony.yeo@smart.mit.edu*, [‡]{*hover,nmp*}*@mit.edu*

***Abstract*—This paper presents a simultaneous localisation and mapping (SLAM) algorithm implemented on an autonomous sea kayak with a commercial off-the-shelf X-band marine radar mounted. The Autonomous Surface Craft (ASC) was driven in an off-shore test site in Singapore's southern Selat Puah marine environment. Data from the radar, GPS and an inexpensive single-axis gyro data were logged by an on-board processing unit as the ASC traversed the environment, which comprised geographical and surface vessel landmarks. An automated feature extraction routine is presented, based on a probabilistic landmark detector, followed by a clustering and centroid approximation approach. With restrictive feature modeling, and a lack of vehicle control input information, it is demonstrated that via the novel RB-PHD-SLAM Filter, useful results can be obtained, despite an actively rolling and pitching ASC on the sea surface. In addition, the merits of investigating ASC SLAM are demonstrated, particularly with respect to the map estimation, obstacle avoidance and target tracking problems. Despite the presence of GPS and gyro data, heading information on such small ASC's is greatly compromised which induces large sensing error, further accentuate by the large range of the radar sensor. This work is a step towards realising an ASC capable of performing environmental or security surveillance and reporting a real-time active awareness of the above-water scene.**

***Index Terms*—Random Finite Set SLAM, Marine Radar, Autonomous Surface Craft**

I. Introduction

The goal of realising a completely autonomous outdoor mobile platform remains a challenging research issue. While autonomy requires multiple task-specific modules, that which is common to all is the ability of the platform to have an active awareness of its working environment, as well as knowing its location at each time with respect to that environment. A precise measurement of the robots surroundings is essential to any task or behaviour the robot may be required to perform. A broad range of exteroceptive sensors are generally deployed on the autonomous vehicle to acquire information about the surrounding area, which measure the relative range and bearing (as well as other properties) from the vehicle to environmental landmarks. Regardless of the choice of sensor to measure the working environment (a marine landscape in this work), such measurements are subject to uncertainty such as measurement noise, detection uncertainty, spurious measurements and data association uncertainty. Stochastic estimation methods have become popular in handling all these sources of uncertainty in the measured data. Furthermore, given the inherent co-dependance of localisation and mapping, their joint estimation became a highly active research field since the seminal developments of smith et. al [1], and the problem became known as Simultaneous Localisation and Mapping (SLAM).

Fig. 1. *The experimental testing ground at Singapore's Selat Puah: A fused satellite / sea-chart overview.*

While the vast majority of SLAM systems operate on grounded land vehicles [2], [3], the operating environment examined in this paper is a marine scenario off the southern coast of Singapore. Figure 1 depicts this scene as sea chart fused with satellite imagery, where the scale of the image is approximately 10km x 10km. The test-site within the scene where trials were carried out is also highlighted. Despite the availability of positional information via GPS with minimal occlusion, performing SLAM with an ASC gives rise to a number of challenging issues, especially when the map estimation component of SLAM is considered. In general, as the mass of water displaced by the surface vessel decreases, the uncertainty of its heading increases, since for a given sea-state,

978-1-4244-7815-6/10/$26.00 ©2010 IEEE

a smaller vessel will pitch roll and yaw more than a bigger vessel. Thus, for a 3m long, 100Kg (fully laden) autonomous sea-kayak (described in section III), heading uncertainty poses a serious concern, particulary when registering the relative measurements to a global frame. Moreover, the smaller size allows for increased maneuverability, introducing frequent sharp turns and non-linear trajectories, adding further challenges to the task of map building and target tracking.

II. Related Work

Investigations into SLAM in a marine environment have received widespread interest over the passed few years, however, almost exclusively in the underwater domain. In [4], a delayed-state SLAM approach was presented and implemented on an underwater vehicle with mounted vision sensors. The approach emulated a structure-from-motion type algorithm from the vision community, using images registered from the estimated vehicle poses to estimate the scene. Fixed sector scan sonar are also a popular choice for underwater robotics applications and are adopted in a number of influential works. A motion estimation and map building algorithm based on a fusion of vision and sector scan sonar data is described in [5]. The approach relied on correlated matches between successive sonar scans and point matches between images to achieve the mostly likely pose of the vehicle. Correlation based methods are commonly adopted in the presence of difficult to model and interpret data, such as that from an unknown and unstructured underwater terrain. Extending the directionality of sector scan sonar of the full 360^o FoV, the mechanically scanned sonar has also been a popular choice. SLAM implementations in a swimming pool using a line-feature approach and scanning sonar were presented in [6]. The study was extended to a semi-structured underwater scenario in [7].

In the grounded autonomous robotics community, radar sensors have been adopted by quite a number of research groups worldwide. The ACFR in Sydney has a long history of working with and designing frequency modulated carrier wave (FMCW) W-band radar for use in mobile robotics. The seminal SLAM work of [2] used a W-band radar sensor for feature based SLAM experimental analysis, while reflectively patterns from leisure craft were examined in [8]. Further SLAM and mapping investigations using W-band radar were presented in [9], [10], [11], [12] examining the signal statistics and their influence on the resulting localisation and map estimates. A scan matching approach for mobile robotics was developed for an FMCW S-band radar in [13], however features were not extracted and jointly estimated with the vehicle pose.

This work therefore extends radar based navigation to a marine environment, presenting a unique addition to the wide range of SLAM implementations. While laser based systems mounted on an ASC, when coupled with suitable algorithms, have proven useful for obstacle avoidance [14], for SLAM investigations, a marine radar represents a natural choice of exteroceptive sensor. To the authors' knowledge, this is the first time that feature-based SLAM has been investigated using a commercial pulsed X-band radar mounted on an ASC. Despite the low mounting height of just 1.5m above the sea-surface, this work demonstrates that the sensor can register land and vessel measurements at ranges of up to 5Km, while performing recursive localisation and map estimation tasks.

III. The Autonomous Surface Craft

This section details the hardware deployed in this work. The ASC is a robotic sea-kayak which represents a low cost, high load bearing platform, being highly maneuverable and capable of operating in shallow waters. For stabilisation in the choppy waters common to Singapore's Selat Puah, lateral buoyancy aids were added to the platform, as depicted in figure 2. The ASC is equipped with a GPS receiver and low cost DSP5000 single-axis gyroscope for 3D pose (x_k, y_k, ϕ_k) measurements at each time k and is drivable / steerable via a rear mounted remote control electric thruster.

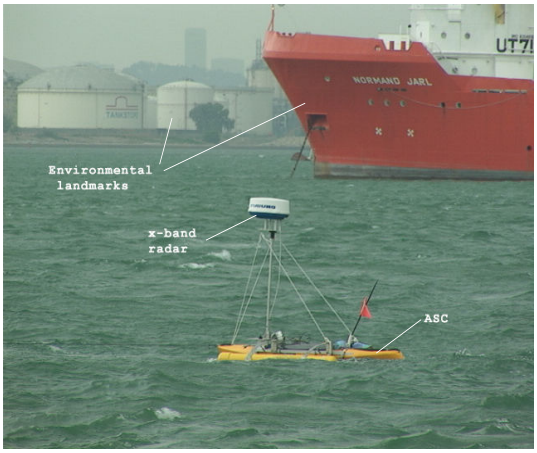

Fig. 2. *The ASC used in the sea trials.*

The X-band sensor mounted on a 1.5m pole, also evident in figure 2, is the M-1832 BlackBox Radar from Furuno powered by an onboard battery. The mechanically scanned beam has a width of 3.9^o in azimuth and 20^o in elevation. The large elevation beamwidth makes the sensor robust to the sometimes severe pitch and roll of the ASC. An onboard processing unit logs the GPS and gyro data at a rate of 1Hz, with the radar data being sampled and logged at a rate of 0.5Hz. Given that the distance traversed by the ASC over a single radar scan is negligible compared to the range (maximum 36 nautical miles) and resolution of the sensor, the issues of distortion with mechanically scanned sensors [6] are considered insignificant.

While the unusually low mounting height of the marine radar undoubtedly increases the sea clutter interference in the logged data, by adopting suitable processing algorithms, the signal can be readily used for recursive localisation and map estimation filters as demonstrated later in section VI. For the trials carried out in this work, the radar range bin resolution, δr, was set to 7.5m, with a maximum range of 7.68Km. An example of a logged radar scan is superimposed on the ground truth image of figure 1 from the measured pose of the ASC at that time and presented in figure 3. The measured GPS data of the ASC trajectory is also shown. Note the (slight, in this

chosen example) angular misalignment due to the poor heading measurement. Reflections from landmarks at distances greater than 5km from the ASC are evident in the data, despite the low mounting height of the sensor. The following section describes the extraction of features from this data for the purpose of performing SLAM.

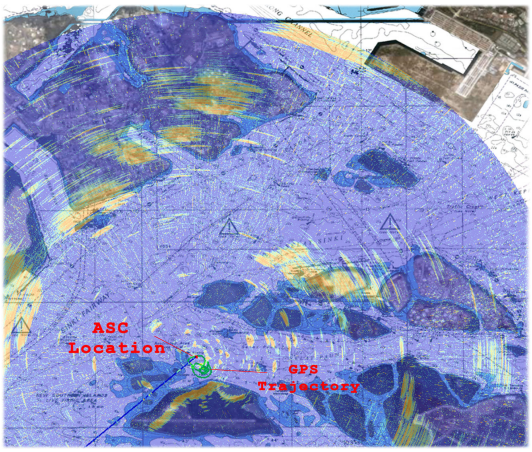

Fig. 3. *A sample measurement from the X-band radar mounted on the ASC.*

IV. Marine Radar Feature Extraction

This section describes the extraction of suitable features from the data depicted in figure 3. Prior to performing feature approximation, the data is first classified into target, $\mathcal{H}_1$ hypothesis, and sea-clutter, $\mathcal{H}_0$ hypothesis, via a stochastic constant false alarm rate detector. Such probabilistic detection methods are based on an underlying assumption on the sea-clutter amplitude statistics. In this work, the amplitude distribution of the sea clutter is obtained empirically by Monte Carlo analysis of over a large number of sample scans, using manually selected windows containing only radar returns from the sea. An adaptive detector is then described to determine the regions of interest in the data. These areas of the data are then smoothed and clustered to extract the feature measurements.

A. Adaptive Detection

If ψ is the received radar signal amplitude, then the empirical sea clutter amplitude, $p(\psi|\mathcal{H}_0)$ can be approximated by an exponential distribution,

$$p(\psi|\mathcal{H}_0) = \begin{cases} \frac{1}{\mu}\exp^{-\psi/\mu} & \text{if } \psi > 0 \\ 0 & \text{Otherwise} \end{cases} \quad (1)$$

as seen in figure 4. While for this trial, the moment μ of the sea clutter amplitude distribution may be empirically estimated, constituting *a priori* information for the feature detection module, in practice, the moment may change depending on the sea state or roll / pitch of the ASC. As such, an adaptive detection method is applied to locally estimate the moment, μ, in each range bin, r, and derive a variable threshold value, T_r.

Figure 4 also shows a sample radar power vs. range spectrum, comprising sea clutter as well as both point (surface craft) and extended (land) targets. Due to the closely lying point targets and to avoid potential target masking, an Ordered Statistics approach is applied where [10], [15],

$$P_{fa} = k_{os}\binom{2W}{k_{os}}\frac{(k_{os}-1)!(\tau+2W-k_{os})!}{(\tau+2W)!} \quad (2)$$

with the threshold value $T_r = \tau\hat{\mu}_r$. τ represents the scaling constant which determines the decision threshold value T_r to achieve a fixed rate of false alarm. $2W$ and k_{os} are constants which represent the sliding window width and the 'k-factor' respectively. The constant τ can then be obtained by non-linear zero finding routines. The resulting threshold across all the range bins for the sample radar spectrum is shown in figure 4, using the parameters, $2W = 40$, $P_{fa} = 0.05$ and $k_{os} = 30$.

As can be seen, the point targets are detected, while most of the land reflections are suppressed. This is because land reflections have the appearance of clutter measurements. This is useful for SLAM applications, since extended targets are more difficult to reliably parameterise as stable features. However, the the resulting map then reflects only point-like objects.

B. Clustering and Feature Extraction

Based on the point target detections from the adaptive threshold, the regions of the measurement data are further examined to assess their likelihood of representing stable features. As can be seen from the measurement data of figure 3, targets rarely occupy a single range bin. Therefore, to suppress the high frequency signal fluctuations which are primarily noise or sea clutter readings, a 2D Gaussian low pass filter is convolved with the regions of the scan identified by the adaptive threshold. The smoothed features are then clustered based on nearby pixels and pruned according to a minimum and maximum area constraints.

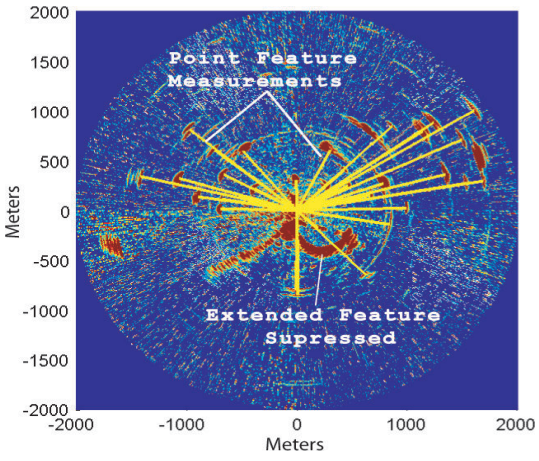

Fig. 5. *Sample point feature measurements (yellow lines) extracted from the raw radar data. These measurements are fed to the SLAM filter for localisation and map building.*

V. SLAM Algorithm

This section describes the feature-based SLAM algorithm implemented and analysed in this paper. Stemming from the

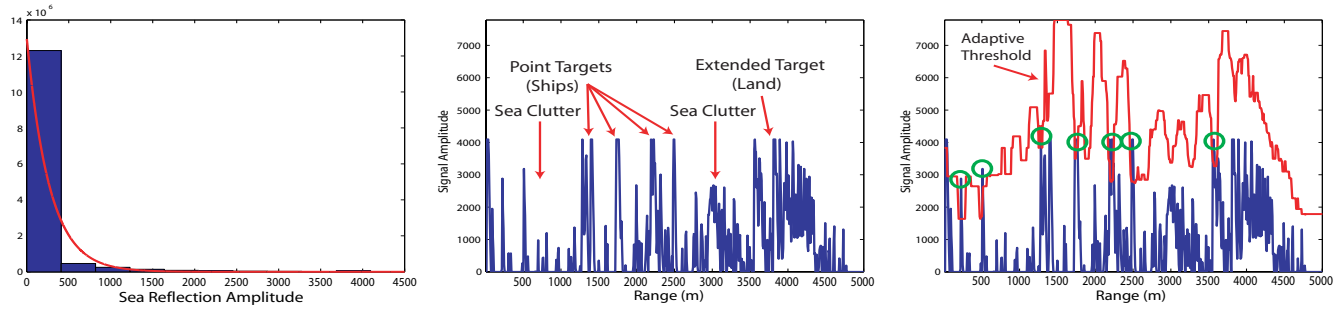

Fig. 4. *Left: The empirical sea-clutter amplitude distribution. Center: A sample radar power vs. range spectrum showing sea clutter, point and extended targets. Right: An adaptive OS-CFAR detection threshold.*

seminal developments in the tracking community [16], [17], recent SLAM investigations suggest that a feature map is more appropriately represented as a *set* of features, requiring the tools of random finite set (RFS) theory [9], [18], [19]. This approach is also adopted in this paper.

A. The Process Model

Unlike ground based vehicles which are generally restricted to forward facing motion dynamics, a sea-based ASC is subject to numerous uncertain disturbances such as currents and wind, moving the ASC in any arbitrary direction. To account for this, the following nonlinear process model is adopted,

$$\begin{aligned} x_{k|k-1} &= x_{k-1} + V_{k-1}\Delta t_k \cos(\phi_{k-1} + \delta\phi_k) + D_x \\ y_{k|k-1} &= y_{k-1} + V_{k-1}\Delta t_k \sin(\phi_{k-1} + \delta\phi_k) + D_y \\ \phi_{k|k-1} &= \phi_{k-1} + \delta\phi_k \end{aligned}$$

Here, D_x and D_y represent random perturbations in the ASC motion due to external sea forces and are modeled by White Gaussian signals. The angular change in orientation, $\delta\phi_k$, is recorded by an on board single axis gyroscope and is assumed corrupted with White Gaussian noise. $\Delta t_k = t_k - t_{k-1}$ is determined from the measurement rate of the gyro. In this investigation, for simplicity, $V_k = V_{k-1}$ and is chosen a priori due to the lack of suitable Doppler Velocity Log sensors. A constant velocity model could also be assumed, and the recursive estimation of V_k integrated into the SLAM algorithm.

B. The Measurement Model

In the system used in this work, the primary exteroceptive measurement sensors is the X-band radar. Such as sensor is prone to missed detections, false alarms, measurement noise and data association uncertainty. To encapsulate such sources of uncertainty, a Random Finite Set measurement model is adopted as,

$$\mathcal{Z}_k = \bigcup_{m\in\mathcal{M}_k} \mathcal{D}_k(m, X_k) \cup \mathcal{C}_k(X_k) \tag{3}$$

which incorporates the feature detections in $\mathcal{D}_k(m, X_k)$ and the spurious measurements in $\mathcal{C}_k(X_k)$. The individual measurements z comprise relative range and bearing measurements from the ASC pose at time k.

C. The Filter

The RFS-SLAM joint posterior can be factorised as,

$$\begin{aligned} p_k(\mathcal{M}_k, X_{0:k}|\mathcal{Z}_{0:k}, U_{0:k-1}, X_0) = \\ p_k(X_{0:k}|\mathcal{Z}_{0:k}, U_{0:k-1}, X_0) p_k(\mathcal{M}_k|\mathcal{Z}_{0:k}, X_{0:k}) \end{aligned} \tag{4}$$

where a Rao-Blackwellised implementation implies the mapping recursion is approximated by a Gaussian Mixture PHD Filter, and the trajectory recursion by a Particle Filter [18]. The calculation of the particle weighting likelihood however, requires the evaluation of,

$$g_k(\mathcal{Z}_k|\mathcal{Z}_{0:k-1}, X_{0:k}) = \int p(\mathcal{Z}_k, \mathcal{M}_k|\mathcal{Z}_{0:k-1}, X_{0:k})\delta M_k$$

which involves a set integral over all possible maps. Note that this likelihood is simply the normalising constant of the Bayes recursion for propagating the RFS map density, $p_k(\mathcal{M}_k|\mathcal{Z}_{0:k}, X_{0:k})$ in (4). The weighting likelihood can then be written,

$$g_k(\mathcal{Z}_k|\mathcal{Z}_{0:k-1}, X_{0:k}) = \frac{g_k(\mathcal{Z}_k|\mathcal{M}_k, X_k) p_{k|k-1}(\mathcal{M}_k|X_{0:k})}{p_k(\mathcal{M}_k|X_{0:k})}.$$

By approximating the predicted and updated RFS map densities as Poisson RFSs according to,

$$p_{k|k-1}(\mathcal{M}_k|X_{0:k}) \approx \frac{\prod_{m\in\mathcal{M}_k} v_{k|k-1}(m|X_{0:k})}{\exp\left(\int v_{k|k-1}(m|X_{0:k})dm\right)} \tag{5}$$

$$p_k(\mathcal{M}_k|X_{0:k}) \approx \frac{\prod_{m\in\mathcal{M}_k} v_k(m|X_{0:k})}{\exp\left(\int v_k(m|X_{0:k})dm\right)}, \tag{6}$$

and setting the dummy variable $\mathcal{M}_k = \emptyset$, a solution was presented and analyzed in [18]. In this paper, an alternative choice of map is used, $\mathcal{M}_k = \{\bar{m}\}$, where $\bar{m}$ is a single feature chosen according to a given strategy. In this case, the weighting likelihood becomes,

$$\begin{aligned} g_k(\mathcal{Z}_k|\mathcal{Z}_{0:k-1}, X_{0:k}) \approx \frac{1}{\Gamma}\Bigg[\Bigg((1 - P_D(\bar{m}|X_k))\kappa_k^{\mathcal{Z}_k} + \\ P_D(\bar{m}|X_k)\sum_{z\in\mathcal{Z}_k} \kappa_k^{\mathcal{Z}_k - \{z\}} g_k(z|\bar{m}, X_k)\Bigg) v_{k|k-1}(\bar{m}|X_{0:k})\Bigg] \end{aligned} \tag{7}$$

with,

$$\Gamma = \exp\left(\hat{\mathfrak{m}}_k - \hat{\mathfrak{m}}_{k|k-1} - \int c_k(z)dz\right) v_k(\bar{m}|X_{0:k}).$$

Here $\hat{\mathfrak{m}}_k$ and $\hat{\mathfrak{m}}_{k|k-1}$ are the estimated and predicted number of features in the explored map $\mathcal{M}_k$, while v_k and $v_{k|k-1}$ are the updated and predicted Probability Hypothesis Density's of the map. The map estimation is handled by a Gaussian Mixture implementation of the PHD predictor,

$$v_{k|k-1}(m|X_{0:k}) = v_{k-1}(m|X_{0:k-1}) + b(m|X_k) \quad (8)$$

where $b(m|X_k)$ is the PHD of the new feature RFS, $\mathcal{B}(X_k)$, and corrector,

$$v_k(m|X_{0:k}) = v_{k|k-1}(m|X_{0:k})\Bigg[1 - P_D(m|X_k) + \sum_{z\in\mathcal{Z}_k} \frac{\Lambda(m|X_k)}{c_k(z|X_k) + \int_{\zeta\in\mathcal{M}_k} \Lambda(\zeta|X_k) v_{k|k-1}(\zeta|X_{0:k})d\zeta}\Bigg] \quad (9)$$

where $\Lambda(m|X_k) = P_D(m|X_k)g_k(z|m, X_k)$ and,

$P_D(m|X_k)$ = the probability of detecting a feature at m, from ASC pose X_k.
$c_k(z|X_k)$ = PHD of the clutter RFS $\mathcal{C}_k$ in (3) at time k.

See [18] for more details.

VI. Experimental Results

This section details the analysis of the SLAM algorithm on an extensive dataset recorded from the test site shown in figure 1. The ASC was taken on a nonlinear trajectory over 1.8Km long, logging over 650 consecutive radar scans at a rate of 0.5Hz in trial run last over 25 minutes. Multiple loops and linear paths were traversed. The analysis focusses first on the location estimates from the SLAM filter, followed by an examination of the estimated map. Monte carlo analysis is presented based on 50 sample runs using 100 trajectory particles in each trial.

A. Positional Estimation Analysis

Figure 6 depicts the estimated ASC trajectory from each for the MC runs in comparison with the GPS data. A sample trajectory from the assumed ASC motion model, using the measured gyroscope data, is also provided. The results demonstrate that the proposed approach can accurately reconstruct the traversed path, despite the sensing and vehicle modeling difficulties. Quantification of the positional error is provided in figure 7, indicating a maximum error of 45m. While this result demonstrates that ASC based SLAM is realisable, further investigations have to be carried out to get positional error comparable to that from GPS.

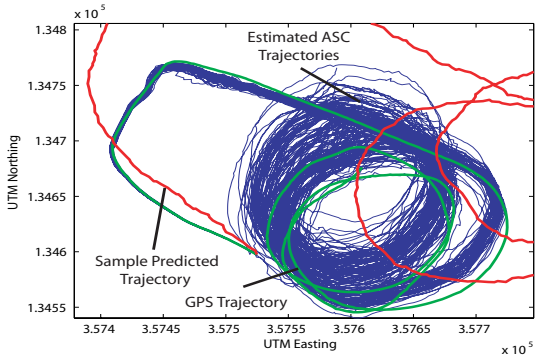

Fig. 6. *The expected trajectories from each of the 50 MC trials (blue), compared to the GPS trajectory (green).*

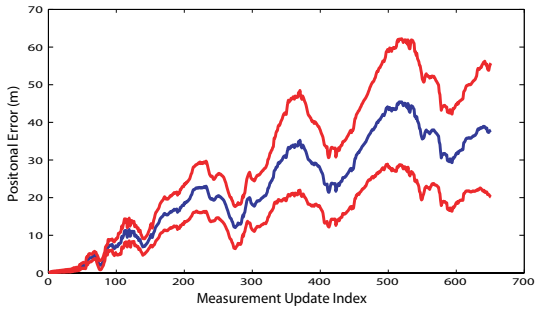

Fig. 7. *Quantification of the mean error in the estimated position (blue) of the ASC by the proposed SLAM system. One sigma standard deviation bounds are also shown (red).*

B. Map Estimation Analysis

Given that the ground truth heading information is unavailable, the quality of the resulting map estimate can be used the gauge the quality of the estimated ASC heading. This is especially suitable given the large sensing range of the radar. Since (most of) the point targets are stationary during the trial, and all of the extended targets (land masses) are stationary, for a given map estimation routine, the quality of the posterior map estimate from the temporal fusion of the measurement data provides an indication of the quality of the pose estimates. Using a simplistic linear function from signal power to Log-Odds occupancy [12], the posterior occupancy grid can be propagated as each X-band radar measurement arrives. A close up snap shot of the posterior map estimates from both a sample predicted trajectory and the estimated trajectory are provided in figures 8 and 9. The fused map from the SLAM method is seen to be far more informative than that from the predicted trajectory, with the island coastline and surface vessels clearly evident.

VII. Conclusion

This paper examined the applicability of SLAM using an autonomous surface craft (ASC) in a marine environment. Adopting a commercial X-band radar as the main exteroceptive sensor, the investigation demonstrated that despite the widespread presence of GPS information at sea, the heading measurements (based on an inexpensive single axis gyroscope)

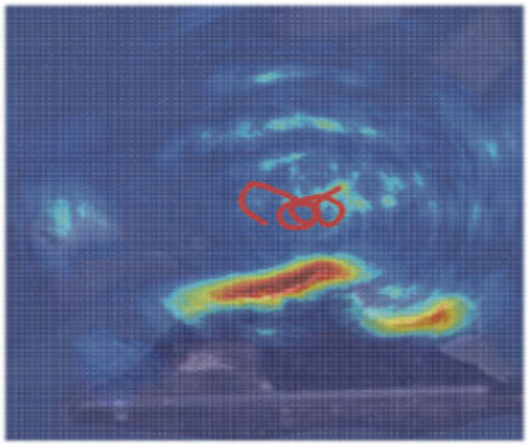

Fig. 8. *The estimated map from the predicted ASC trajectory, in comparison to satellite and sea chart imagery. An uninformative map is evident given the poor pose estimates.*

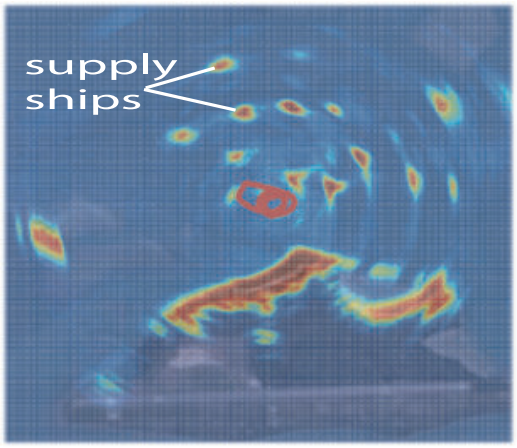

Fig. 9. *The estimated map from the proposed SLAM algorithm, in comparison to satellite and sea chart imagery. The map be seen to coincide well with the islands present as well as a surface vessels. Unfortunately the GPS information from supply ships (evident in figure 1) in the area was unavailable at the time.*

can still be prone to large error. Considering the large range of the sensor, this resulted in uninformative map estimates, limiting the applicability of the craft to tasks such as autonomous mapping, obstacle avoidance and surface craft tracking.

Based on an automatic point target detector, a Random Finite Set feature based simultaneous localisation and mapping algorithm was developed to recursively estimate the ASC location and heading, as well as build the map. The point targets exploited were anchored supply ships and buoys present in the test site. The algorithm demonstrated how useful results are realisable, even with difficult to model vehicle dynamics and a lack of any input control measurements. Comparisons of the estimated maps demonstrates the merits of SLAM for an ASC, given uncertainty heading and sensor measurements information. Future work will incorporate the extended land targets, as well as examine joint mapping and target tracking from an ASC.

ACKNOWLEDGEMENT

This research is funded in part by the Singapore National Research Foundation through the Singapore-MIT Alliance for Research and Technology CENSAM.

REFERENCES

[1] R. Smith, M. Self, and P. Cheeseman. A stochastic map for uncertain spatial relationships. In *the fourth international symposium of Robotics Research*, pages 467–474, 1987.

[2] G. Dissanayake, P. Newman, H.F. Durrant-Whyte, S. Clark, and M. Csorba. A solution to the simultaneous localization and map building (SLAM) problem. *IEEE Transactions on Robotic and Automation*, 17(3):229–241, June 2001.

[3] S. Thrun. Robotic mapping: A survey. Technical Report CMU-CS-02-111, Carnegie Mellon University, Pittsburgh, Pennsylvania 15213, February 2002.

[4] R.M. Eustice, H. Singh, and J.J. Leonard. Exactly sparse delayed-state filters for view-based slam. *IEEE Transactions on Robotics*, 22(6):1100–1114, December 2006.

[5] B. Kalyan, A. Balasuriya, H. Kondo, T. Maki, and T. Ura. Motion estimation and mapping by autonomous underwater vehicles in sea environments. In *Proceedings of IEEE Oceans*, pages 436–441, 2005.

[6] D. Ribas, P. Ridao, J. Niera, and J.D. Tardos. Slam using an imaging sonar for partially structured underwater environments. In *IEEE/RSJ International Conference on Intelligent Robots and Systems (IROS)*, October 2006.

[7] D. Ribas, P. Ridao, J.D. Tardos, and J. Niera. Underwater slam in a marina environment. In *IEEE/RSJ International Conference on Intelligent Robots and Systems (IROS)*, San Diego, CA, October 2007.

[8] G. Brooker, C. Lobsey, and R. Hennessy. Low cost measurement of small boat rcs at 94ghz. In *Proceedings of IEEE International Conference on Control, Automation and Robotics*, 2006.

[9] J. Mullane, B.N. Vo, M. Adams, and W.S. Wijesoma. A random set approach to slam. In *proceedings of the IEEE International Conference on Robotics and Automation (ICRA) workshop on Visual Mapping and Navigation in Outdoor Environments*, Japan, May 2009.

[10] J. Mullane, M. Adams, and W.S. Wijesoma. Robotic mapping using measurement likelihood filtering. *International Journal of Robotics Research*, 2(28):172–190, 2009.

[11] E. Jose, M.D. Adams, J. Mullane, and N. Patrikalakis. Predicting millimetre wave radar spectra for autonomous navigation. *IEEE Sensors Journal*, 10(5):960–971, May 2010.

[12] A. Foessel, J. Bares, and W.R.L. Whittaker. Three-dimensional map building with MMW RADAR. In *Proceedings of the 3rd International Conference on Field and Service Robotics*, Helsinki, Finland, June 2001. Yleisjljenns - Painnoprssi.

[13] F. Gerossier, P. Checchin, C. Blanc, R. Chapuis, and L. Trassoudaine. Trajectory-oriented EKF-SLAM using the fourier-mellin transform applied to microwave radar images. In *Proceedings of the IEEE/RSJ International Conference on Intelligent Robots and Systems*, MO, USA, October 2009.

[14] T.Bandyophadyay, L. Sarcione, and F. Hover. A simple reactive obstacle avoidance algorithm and its application in singapore harbor. In *Proceedings of the 7th International Conference on Field and Service Robotics*, MA, USA, 2009.

[15] H. Rohling. Radar cfar thresholding in clutter and multiple target situations. In *IEEE Transactions, AES-19*, pages 608–621, 1983.

[16] B.N. Vo, S. Singh, and A. Doucet. Sequential monte carlo methods for multi-target filtering with random finite sets. *IEEE Transactions on Aerospace and Electronic Systems*, 41(4):1224–1245, October 2005.

[17] B.N. Vo and W.K. Ma. The gaussian mixture probability hypothesis density filter. *IEEE Transactions on Signal Processing*, 54(11):4091–4104, November 2006.

[18] J. Mullane, B.N. Vo, and M. Adams. Rao-blackwellised PHD SLAM. In *proceedings of the IEEE International Conference on Robotics and Automation (ICRA)*, Alaska, USA, May 2010.

[19] J. Mullane, B.N. Vo, M. Adams, and W.S. Wijesoma. A random set formulation for bayesian slam. In *proceedings of the IEEE/RSJ International Conference on Intelligent Robots and Systems*, France, September 2008.